Sensors & Actuators: B. Chemical 286 (2019) 237–242

Contents lists available at ScienceDirect

Sensors and Actuators B: Chemical

journal homepage: www.elsevier.com/locate/snb

Electrochemical graphene/carbon nanotube yarn artificial muscles

Jae Sang Hyeon[a], Jong Woo Park[a], Ray H. Baughman[b], Seon Jeong Kim[a,*]

[a] Center for Self-Powered Actuation, Department of Biomedical Engineering, Hanyang University, Seoul, 04763, South Korea
[b] The Alan G. MacDiarmid NanoTech Institute, The University of Texas at Dallas Richardson, TX, 75080, USA

ARTICLE INFO

Keywords:
Artificial muscles
Carbon nanotubes
Graphene
Electrochemical actuators
Supercapacitors

ABSTRACT

Fiber-type artificial muscles similar to natural muscles are being studied for applications such as robots, prosthetics and exoskeletons. In particular, carbon nanotube (CNT) yarn artificial muscles have attracted interest for their unique mechanical and electrical properties as electrochemical artificial muscles. Here, we demonstrate the large tensile stroke of CNT-based electrochemical yarn artificial muscles induced by increasing capacitance. The coiled graphene/CNT yarns made by the biscrolling method can produce greater tensile actuation using more ions at the same voltage than pristine CNT coils. The maximum tensile actuation of these electrochemical muscles is 19%, which is two times larger than coiled CNT muscles with a work capacity of 2.6 J g^{-1}. These electrochemical artificial muscles could be further developed for practical applications, such as micromechanical devices and robotics.

1. Introduction

Artificial muscles that contract and expand like natural muscles are needed to realize the natural movement of human-like robots or exoskeletons. Among various artificial muscles, electrochemical artificial muscles have the potential for higher energy conversion efficiency and better controllability. Many kinds of electrochemical actuators, such as nanoporous metals [1–9], conducting polymers [10,11], ionic polymer metal composites [12–17], and carbon nanotubes [18–22] (CNTs) have been reported.

CNT yarns made by inserting a twist into CNT sheets have excellent mechanical and electrical properties, high surface area and light weight, and thus can achieve high performance as electrochemical artificial muscles. Since the report of the electrochemical torsional actuation from twisted CNT yarns in 2011 [20], the self-coiled CNT made by inserting more twists, showed a contraction movement as an all-solid-state tensile muscle in air [21]. Recently, it has been shown that two-ply coiled CNT yarns produce tensile strokes as high as −16%, ≈30 times higher work capacity than natural muscles by applying a voltage of −3.25 V [22].

The electrochemical CNT artificial muscles are basically supercapacitors based on electrochemical double-layer charge injection, and the ions from the electrolyte enter the pore space within the yarns, thereby causing the untwisting and contraction with volume expansion of yarns. Therefore, to obtain high actuator strains at the same voltage, a high capacitance, which means that a large number of ions are used for actuation, is one of the key factors for electrochemical artificial muscles [23].

CNT yarns can contain guest materials by biscrolling [24], to achieve other purposes such as biofuel cells that transfer electrons from biomolecules [25] or as artificial muscles that respond to various stimuli like heat [26], humidity [27] and biomolecules [28]. In addition, some guest materials, such as conducting polymers [29,30] and metal oxides [31], provide capacitance enhancement for CNT yarn supercapacitors. By adjusting the loading amount of the guest materials when making the biscrolled CNT supercapacitors, it is possible to control the trade-off relationship between the capacitance for the energy storage performance and the mechanical strength for flexibility and stretchability [31].

Here, we demonstrate the larger tensile stroke of coiled CNT muscles using biscrolled guest materials to increase the capacitance. Graphene as a guest material of CNT yarn increases the capacitance of the whole artificial muscle system and induces more than two times higher tensile strokes than pristine CNT coils at −3 V with the cation, tetrabutylammonium (TBA) ion.

2. Materials and methods

2.1. Materials

Multiwalled carbon nanotube (MWNT) sheets were directly drawn from an MWNT forest that was grown on a Si wafer by chemical vapor

* Corresponding author.
E-mail address: sjk@hanyang.ac.kr (S.J. Kim).

https://doi.org/10.1016/j.snb.2019.01.140
Received 5 November 2018; Received in revised form 28 December 2018; Accepted 27 January 2019
Available online 30 January 2019

deposition of acetylene gas (U053HANYANG-SH158-06, Nano-Science & Technology Center, LINTEC of America Inc.). Tetrabutylammonium hexafluorophosphate (TBA•PF_6, M_w: 387.43 g mol^{-1}), propylene carbonate (PC, anhydrous, 99.7%), and poly(vinylidene fluoride-co-hexafluoropropylene) (PVDF-co-HFP, M_w: ≈455,000, M_n: ≈110,000, pellets) were purchased from Sigma-Aldrich (USA). Graphene dispersion in NMP (50 mg ml^{-1}) was purchased from Graphene Platform Corporation (Japan).

2.2. Preparation of electrolytes, reference and counter electrodes

Liquid electrolyte was prepared by dissolving TBA•PF_6 TBA·PF_6 in PC (50 ml) to a concentration of 0.2 M. To obtain a gel electrolyte, a solution containing both electrolyte and polymer was prepared as follows: acetone (30 g) and PVDF-co-HFP (3 g) were mixed in a stirred oil bath for 2 h at 60 °C. After diluting the polymer concentration to 1 wt%, the PVDF-co-HFP/acetone solution was mixed with 0.5 M TBA•PF_6 TBA·PF_6 in PC to obtain a volume ratio of 1:5. The solvent was evaporated at room temperature for about 2 h to obtain gel electrolytes. Non-aqueous Ag/Ag^+ reference electrode (MW-1085) purchased from BASi Corporation (USA) for three-electrode experiments, and CNT sheets embedded Pt mesh was used as high-surface-area counter electrode [22].

2.3. Fabrication of coiled graphene/CNT yarns for tensile artificial muscles

CNT sheets (10 cm long and 2 cm wide) were stacked and twisted ≈800 turns/m to make yarn structure in graphene solution that was dispersed in NMP using ultrasonication (1 h at 150 W, VCX 750). The concentrations of graphene solutions are 25 and 15 mg ml^{-1} for 80 and 50 wt% graphene/CNT yarns, respectively. After removal from the solution, they were further twisted under a constant load, using a motor, until fully coiled (≈3500 turns/m). To make the similar diameter for all sample to compare the performance, 3, 5 and 15 stacks of CNT sheets were used for 80, 50 wt% graphene/CNT, and pristine CNT muscles respectively. The weight of the graphene was calculated by subtracting the weight of used CNT sheets from the total sample weight.

2.4. Characterization

An actuating working electrode, a coiled yarn muscle connected by a Pt wire at one end, was immersed in 0.2 M TBA•PF_6/PC liquid electrolyte along with a Pt/CNT counter electrode and Ag/Ag + reference electrode in a three-electrode system. In a two-electrode system, a pair of symmetric yarns were prepared, and one was used as a working electrode and the other was used as a counter electrode with 0.5 M TBA•PF_6/PC/PVDF-co-HFP gel electrolyte. At the other end of the actuating working electrode, a thermomechanical analyzer (TMA, SS7100) was attached for applying force and measuring the tensile stroke. The percentage of tensile actuation is calculated by dividing the increased length by the loaded length of the muscle. Voltage and current were measured using a Gamry potentiostat (Reference 600 +). The mechanical properties were measured using a universal testing machine (UTM, Shimadzu model: EZ-SX, Japan).

3. Results and discussion

3.1. Electrochemical graphene/CNT artificial muscles

The MWNT yarns have high strength and toughness that are enough for coiled yarns, but when they include other guest materials with high loading level, too high a stress causes breakage of the graphene/CNT yarns before they become coiled yarns. In addition, as the weight percent of graphene for the graphene/CNT yarn artificial muscles increases, the mechanical properties that depend on the MWNT bundles of the muscles decrease (Fig. S1). Obtaining high tensile actuation from graphene that allows the capacitance increase of electrochemical muscles is interesting, but to lift a heavier load, high mechanical performance is required in artificial muscles. For the above reasons, the amount of graphene contained in the CNT muscles needs to be optimized. Experimentally, coiled graphene/CNT muscles could be made up to 80 wt% of graphene, and if they contained more than that, the twisted yarns were broken.

The large ion size, as well as the high potential range of the organic electrolyte, is a positive factor for the expansion of the electrochemical artificial muscles. A negative potential range was applied to show the large stroke of electrochemical artificial muscles because the cation in this electrolyte, TBA, is more than four times larger than the anion. However, in the previous research [22], the contraction of the CNT artificial muscles was not completely proportional to the ion size because of higher capacitance with small ion. That is, as the size of the ion increases, the number of ions involved in the electrochemical reaction is small, so that the driving of the artificial muscle does not increase as expected for the ion size. Therefore, the improvement of the capacitance may produce a higher actuation for electrochemical CNT muscles in the same electrolyte based on the increase in the number of charged ions.

When the coiled muscles generate tensile strokes with applied electricity, some rotation also occurs even though both ends of the yarns are tethered (Fig. 1B) [20]. This electrochemically driven movement was measured by a thermomechanical analyzer (TMA) reversibly in response to the input triangle wave voltages of cyclic voltammetry (Fig. 1C). The CNT muscle containing graphene also shows a reversible actuation at various scan rates as in previous reports of CNT artificial muscles (Fig. 1D).

3.2. Electrochemical tensile actuation of coiled grpahene/CNT and bare CNT muscles

The contraction of graphene/CNT yarn actuators follows the general tendency for the change of stress produced by the weight to be lifted (Fig. 2A). At a low stress, the contact between adjacent coils interferes with contraction of the actuators, and as the weight applied to the coiled yarns increases, the space between adjacent coils becomes enough to permit high-tensile actuation of the artificial muscles [32]. After the stress at which the maximum stroke occurs, the free space remains between the coils, but as the spring index changes with increasing length of the coils by heavy weights, the contraction movement of artificial muscles decreases [33]. The stress range at which the maximum stroke of the artificial muscle occurs varies with the mechanical strength of the yarn, which depends on the amount of graphene contained in the CNT muscles. To confirm the mechanical and electrochemical effects of the graphene as electrochemical artificial muscles, all coiled samples, from the pristine CNT to the graphene/CNT yarns with a high percentage of guest materials, were made with similar diameter and spring index to minimize the difference in physical factors, such as transfer distance of ions and correlation coefficient between volume expansion and length contraction of yarns. The larger the amount of graphene included in the CNT yarns, the smaller the amount of nanotube sheets used to maintain the same diameter, thereby reducing the weight of loads required to make the coil structure for the same spring index. The maximum tensile actuations are 8.7, 12 and 19.4% for bare CNT, 50 wt% graphene/CNT and 80 wt% graphene/CNT muscles at 17.1, 12.6 and 3.87 MPa, respectively. The stresses are normalized to the cross-sectional area of yarns, using the inner diameter of the coiled yarns. As the maximum contraction of yarn artificial muscles is increased by graphene, the optimal weights go down because the physical performance is decreased by the reduced fraction of CNTs. Therefore, the work capacity, which is calculated from the lifted load and length change, has similar values for both coiled graphene/CNT and bare CNT muscles because of the trade-off between the tensile actuation and the stress range (Fig. S2).

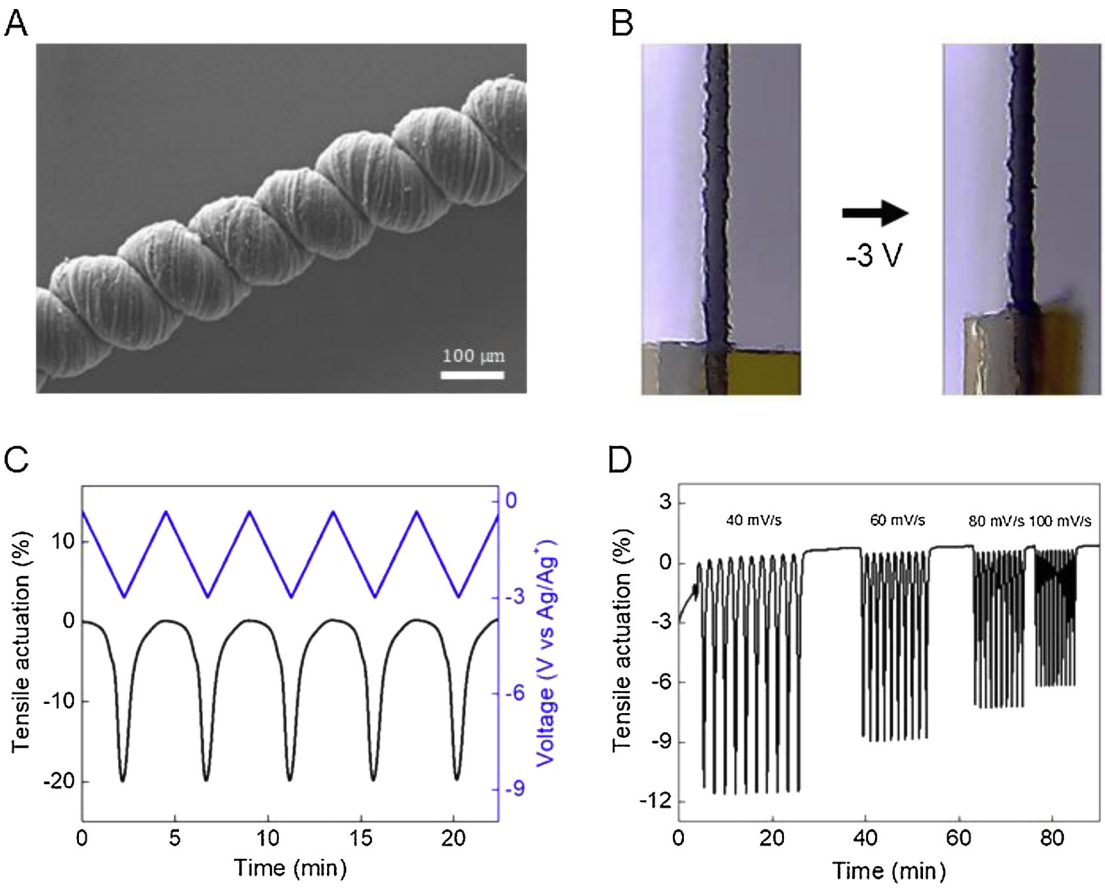

Fig. 1. Coiled graphene/CNT yarns and their electrochemical actuation. (A) SEM image of coiled graphene/CNT yarn. The inner diameter of the coiled yarn is ≈100 μm and the outer diameter is ≈160 μm (scale bar, 100 μm). (B) Optical images showing the actuation of a coiled graphene/CNT yarn muscle in the 0.2 M TBA•PF_6 TBA·PF_6 liquid electrolyte when −3 V is applied. Kapton tape shows the contraction and rotation of the yarn. Applied stress is ≈4 MPa by TMA. (C) The time dependence of applied voltage and resulting tensile actuation of a coiled graphene/CNT yarn when the voltage scan rate is 20 mV s^{-1}. (D) Tensile actuation versus time at different scan rates: 40, 60, 80 and 100 mV s^{-1}.

As the scan rate increases, the number of charges that can be used for driving the electrochemical artificial muscles decreases, so that the tensile strokes are reduced with storage capacity (Fig. 2B, S3). When graphene is included, the retention of capacitance versus scan rate is ≈0.6, which is lower than the ≈0.7 of bare CNT yarns. As a result, graphene/CNT muscles have a larger performance decrease with increasing scan rate than CNT muscles. In particular, at 100 mV s^{-1}, the actuation percent is nearly equal to ≈7%, although the specific capacitance of graphene/CNT muscles is 22.5 F g^{-1}, still 2.6 times higher than pristine CNT muscles. This phenomenon suggests that graphene/CNT artificial muscles are physically disturbed in the tensile movement from graphene and that the effect of physical disturbance is predominant in reducing the capacitance effect as the scan rates increase. In contrast to the scan rate, as the voltage range increases, the actuation improvement by graphene is even more noticeable (Fig. 2C). When a triangle wave voltage is applied from 0 to −1 V, the tensile strokes are -0.03 and -0.05% for coiled pristine CNT and 80 wt% graphene/CNT muscles, respectively, and if the voltage range increases to −3 V, it increases to the highest performance for each, 8.7 and 19.4%, respectively.

3.3. Charge-induced tensile actuation of coiled grpahene/CNT and bare CNT muscles

In addition to the increase in the number of ions by graphene, the volume expansion of the graphene itself during charge storage is also a possible factor in the contribution of tensile strokes. However, the volume expansion of graphene by charge injection is lower than 1% [34], and when guest material expands ≈20%, only ≈1.5% of tensile actuation for coiled CNT yarns occurs [26]. Therefore, there is almost no effect of graphene expansion, and the large contraction is due to an increase in the number of intercalated ions. The volumetric capacitance increases up to a maximum 1.6 times, at which time the tensile contraction was increased 2.3 times by graphene (Fig. 2D). The capacitance for the yarns was calculated from the integral of the cyclic voltammetry (CV) curve in Fig. 3A. The half area of CV was divided by scan rate and voltage range to obtain capacitance. Because the length contraction is due to the expansion by incoming charge into yarns, it is most appropriate to use volume to normalize for equality comparisons. The volume of the coiled yarn was calculated as a cylinder, using the outer diameter of the coil. When graphene is included in the CNT yarns, an abrupt current increase, which implies some chemical reaction, occurs around −3 V, which may cause some errors in the capacitance calculation. Further research is needed to determine whether these unexpected current tails affect the driving of electrochemical artificial muscles.

At the same voltage, the graphene/CNT yarns can store more charge, which in this case means that it has more TBA cations than bare CNT yarns (Fig. 3B). As more ions are used for contraction, the artificial muscles can move more at the same voltage; however, when the same charge amount is involved, the bare CNT generates more tensile movement than graphene/CNT with larger capacitance (Fig. 3C). This result also suggests, with the scan rate result (Fig. 2B), that in addition to the effect of increasing the capacitance by graphene, there is some physical interference with actuation from graphene. The enhancement of the tensile actuation on the graphene/CNT muscles is due to an increase in charge, which is a result of an increase in the input electrical

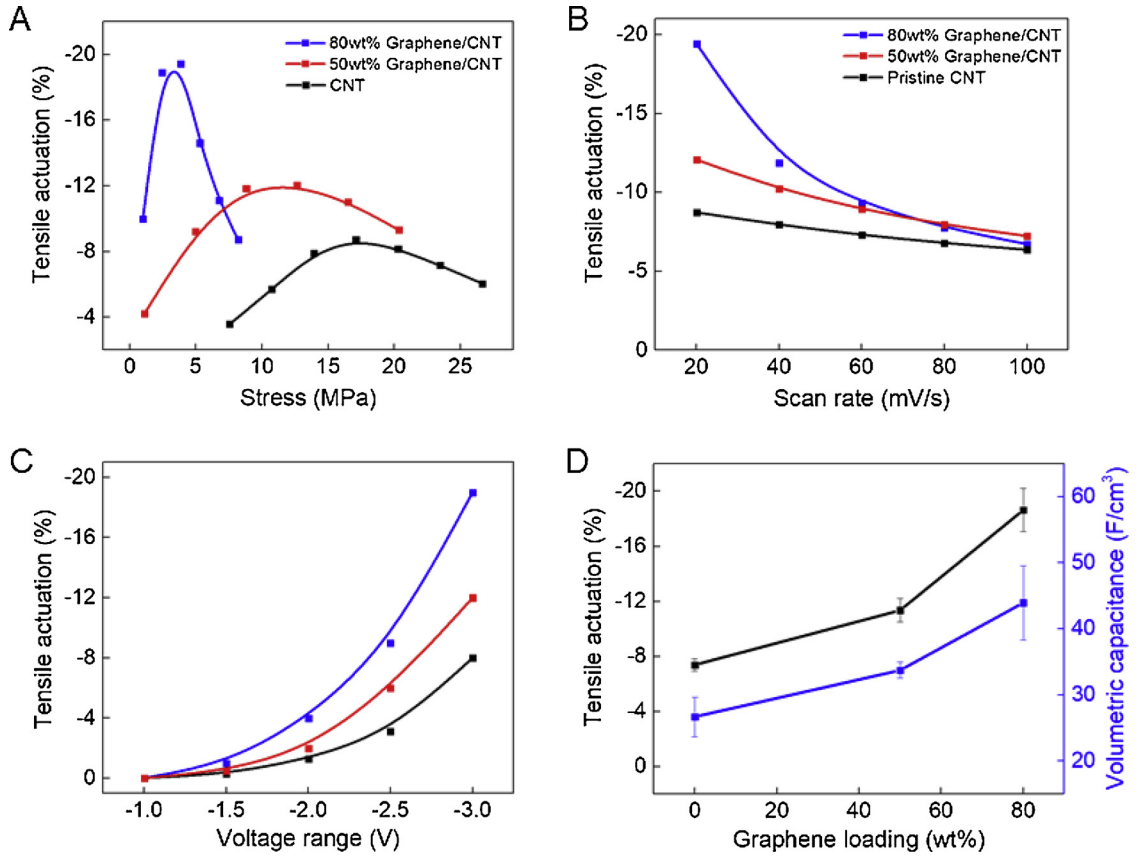

Fig. 2. Electrochemical tensile actuation of coiled graphene/CNT yarns and bare CNT yarn under cyclic voltammetry scan. (A) Tensile actuation versus the applied stress of graphene/CNT yarns and a CNT yarn. Potential range is 0 to −3 V, and scan rate is 20 mV s^{-1}. (B) Tensile actuation versus scan rate of the graphene/CNT yarns and CNTHE THE CNT yarn. Potential range is 0 to −3 V, and applied stress is 4 (blue), 12 (red) and 17 (black) MPa. (C) Tensile actuation versus the potential range of the graphene/CNT yarns and CNT yarn. Scan rate is 20 mV s^{-1}, and applied stress is 4 (blue), 12 (red) and 17 (black) MPa. (D) Optimized tensile actuation and volumetric capacitance of several CNT-based yarns with different graphene wt%. The error bars show the s.d. for three cases. (For interpretation of the references to colour in this figure legend, the reader is referred to the web version of this article).

energy at the same voltage. Therefore, as the input electrical energy increases, it can be expected to be lower than the pristine CNT muscles in terms of energy conversion efficiency.

3.4. All-solid-state graphene/CNT yarn muscles

For a more practical approach, the weight and volume of the overall actuation system should be smaller [21]. In Fig. 4A, the solid gel electrolyte, poly(vinylidene fluoride-co-hexafluoropropylene) (PVdF-co-HFP) containing 0.5 M TBA•PF_6 TBA·PF_6 /PC was used to show the actuation performance without liquid electrolyte, leading to low volumetric performance for the total actuating system. In addition, in the case of a solid electrolyte, the two-electrode system was used for a compact system, in which a pair of symmetric electrodes were prepared, and one was used as a counter electrode and the contraction of the other was measured. The working electrode used a negative voltage versus the counter electrode yarn so as to use the larger cations for tensile actuation as before. However, due to the difference in the size of

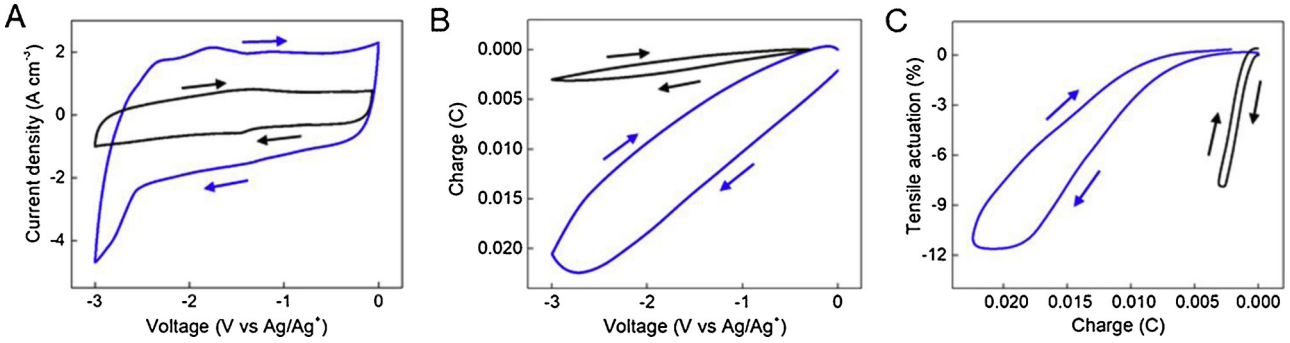

Fig. 3. Electrochemical performance and charge-induced tensile actuation of coiled 50 wt% graphene/CNT yarn (blue) and bare CNT yarn (black) in 0.2 M TBA•PF_6 TBA·PF_6. (A) Cyclic voltammograms of a coiled graphene/CNT yarn and a CNT yarn at scan rates of 20 mV s^{-1}. The refence electrode is Ag/Ag^+ and counter electrode is Pt mesh/CNT. (B) Amount of accumulated charge versus voltage in the coiled graphene/CNT yarn and the CNT yarn, calculated from cyclic voltammograms (A). (C) Electrochemical tensile actuation of the coiled graphene/CNT yarn and the CNT yarn versus penetrated charge. (For interpretation of the references to colour in this figure legend, the reader is referred to the web version of this article).

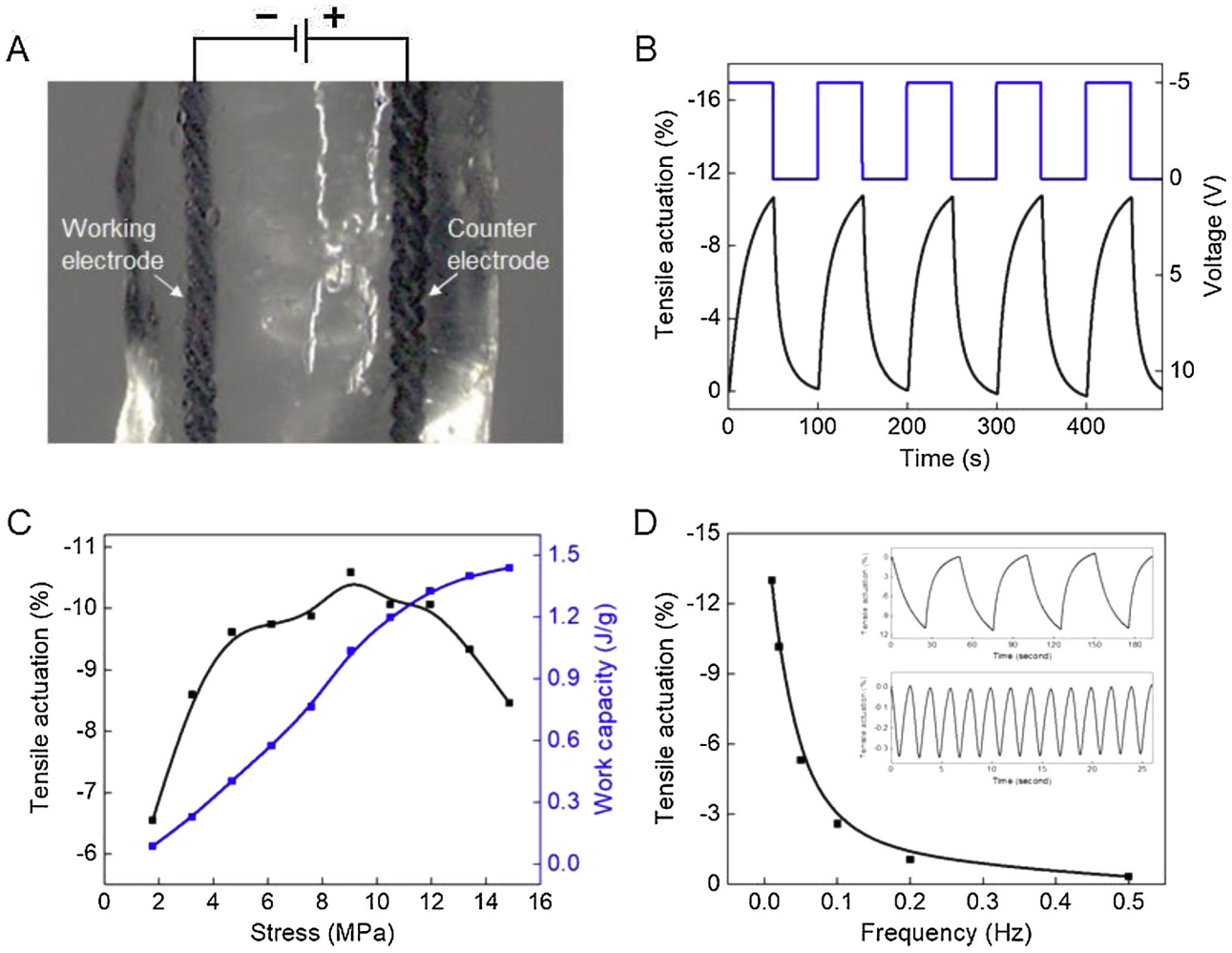

Fig. 4. Electrochemical tensile actuation of coiled 50 wt% graphene/CNT yarns under square wave voltage in a gel electrolyte. (A) Optical microscope images of two-electrode coiled yarns in 0.5 M TBA•PF_6/PC/PVDF-co-HFP gel electrolyte. The thickness of the gel electrolyte is ≈2 mm. (B) The time dependence of the applied voltage and resulting tensile actuation of a coiled graphene/CNT yarn when the voltage is −5 V and the frequency is 0.01 Hz with 50% duty cycle. (C) Tensile actuation and work capacity versus the stress of the graphene/CNT yarns. The applied voltage is −5 V, and the frequency is 0.01 Hz. (D) Tensile actuation versus frequency of the graphene/CNT yarns and CNT yarn. Inset: Tensile actuation versus time when the frequency is 0.02 and 0.5 Hz.

cations and anions, asymmetric actuation occurs in the total device that includes working and counter electrodes and also, the actuation of devices does not reach the actuation of negative electrode, measured in these experiments. The maximum tensile actuation of graphene/CNT muscles in the gel electrolyte is ≈12% using a −5 V, 0.01 Hz square wave voltage with 50% duty cycle, and maximum work capacity is ≈1.5 J g^{-1} when the applied stress is ≈15 MPa (Fig. 4C). As the input frequency increased, the percent of tensile actuation decreased rapidly, and dropped to ≈2.6% at 0.1 Hz (Fig. 4D). This sharp decrease of actuation may be due to slow reaction speed from lower ion mobility and the presence of thick solid electrolyte.

4. Conclusions

In conclusion, we have demonstrated electrochemical tensile CNT artificial muscles with graphene that provide higher capacitance and tensile stroke. Large tensile actuation (≈19%) with graphene is ≈2.5 times higher than the ≈8% of coiled bare CNT muscle at −3 V with a three-electrode system. Although the lifting loads for bare CNT muscles are heavier, graphene/CNT muscles can provide similar work capacity (2.6 J g^{-1}) with large actuation. These tensile actuation and work capacity are higher than previous two-ply coiled CNT muscles, that structurally have improved performance [22]. In addition, performance enhancements through biscrolled graphene have the potential to yield higher performance with previous structural improvements. These electrochemical artificial muscles could be further developed for practical applications, such as micromechanical devices and robotics.

Acknowledgements

This work was supported by the Creative Research Initiative Center for Self-powered Actuation in National Research Foundation of Korea. Support at the University of Texas at Dallas was provided by Air Force Office of Scientific Research grants FA9550-15-1-0089, and the Robert A. Welch Foundation grant AT-0029.

Appendix A. Supplementary data

Supplementary material related to this article can be found, in the online version, at doi:https://doi.org/10.1016/j.snb.2019.01.140.

References

[1] J. Weissmüller, R.N. Viswanath, D. Kramer, P. Zimmer, R. Würschum, H. Gleiter, Charge-induced reversible strain in a metal, Science 300 (2003) 312–315.
[2] D. Kramer, R.N. Viswanath, J. Weissmüller, Surface-stress induced macroscopic bending of nanoporous gold cantilevers, Nano Lett. 4 (2004) 793–796.
[3] H.J. Jin, S. Parida, D. Kramer, J. Weissmüller, Sign-inverted surface stress-charge response in nanoporous gold, Surf. Sci. 602 (2008) 3588–3594.

[4] H.J. Jin, X.L. Wang, S. Parida, K. Wang, M. Seo, J. Weissmüller, Nanoporous Au–Pt alloys as large strain electrochemical actuators, Nano Lett. 10 (2010) 187–194.
[5] E. Detsi, S. Punzhin, J. Rao, P.R. Onck, J.T.M. De Hosson, Enhanced strain in functional nanoporous gold with a dual microscopic length scale structure, ACS Nano 6 (2012) 3734–3744.
[6] J. Zhang, Q. Bai, Z. Zhang, Dealloying-driven nanoporous palladium with superior electrochemical actuation performance, Nanoscale 8 (2016) 7287–7295.
[7] C. Cheng, J. Weissmüller, A.H. Ngan, Fast and reversible actuation of metallic muscles composed of nickel nanowire-forest, Adv. Mater. 28 (2016) 5315–5321.
[8] M. Acerce, E.K. Akdoğan, M. Chhowalla, Metallic molybdenum disulfide nanosheet-based electrochemical actuators, Nature 549 (2017) 370–373.
[9] K. Wanga, C. Stenner, J. Weissmüller, A nanoporous gold-polypyrrole hybrid nanomaterial for actuation, Sens. Actuators B: Chem. 248 (2017) 622–629.
[10] W. Lu, A.G. Fadeev, B. Qi, E. Smela, B.R. Mattes, J. Ding, G.M. Spinks, J. Mazurkiewicz, D. Zhou, G.G. Wallace, D.R. MacFarlane, S.A. Forsyth, M. Forsyth, Use of ionic liquids for π-conjugated polymer electrochemical devices, Science 297 (2002) 983–987.
[11] W. Lu, I.D. Norris, B.R. Mattes, Electrochemical actuator devices based on polyaniline yarns and ionic liquid electrolytes, Aust. J. Chem. 58 (2005) 263–269.
[12] K. Oguro, Y. Kawami, H. Takenaka, Bending of an ion-conducting polymer film-electrode composite by an electric stimulus at low voltage, J. Micromach. Soc. 5 (1992) 27–30.
[13] M. Shahinpoor, Conceptual design, kinematics and dynamics of swimming robotic structures using ionic polymeric gel muscles, Smart Mater. Struct. 1 (1992) 91–94.
[14] D.Z. Zhou, G.M. Spinks, G.G. Wallace, C. Tiyapiboonchaiya, D.R. MacFarlane, M. Forsyth, J.Z. Sun, Solid state actuators based on polypyrrole and polymer-in-ionic liquid electrolytes, Electrochim. Acta 48 (2003) 2355–2359.
[15] B.J. Akle, D.J. Leo, Single-walled carbon nanotubes—ionic polymer electroactive hybrid transducers, J. Intell. Mater. Syst. Struct. 19 (2008) 905–915.
[16] S. Liu, Y. Liu, H. Cebeci, R.G. de Villoria, J.H. Lin, B.L. Wardle, Q.M. Zhang, High electromechanical response of ionic polymer actuators with controlled-morphology aligned carbon nanotube/nafion nanocomposite electrodes, Adv. Funct. Mater. 20 (2010) 3266–3271.
[17] L. Lu, J. Liu, Y. Hu, Y. Zhang, H. Randriamahazaka, W. Chen, Highly stable air working bimorph actuator based on a graphene nanosheet/carbon nanotube hybrid electrode, Adv. Mater. 24 (2012) 4317–4321.
[18] R.H. Baughman, C. Cui, A.A. Zakhidov, Z. Iqbal, J.N. Barisci, G.M. Spinks, G.G. Wallace, A. Mazzoldi, D. De Rossi, A.G. Rinzler, O. Jaschinski, S. Roth, M. Kertesz, Carbon nanotube actuators, Science 284 (1999) 1340–1344.
[19] T. Mirfakhrai, J. Oh, M. Kozlov, E.C.W. Fok, M. Zhang, S. Fang, R.H. Baughman, J.D.W. Madden, Electrochemical actuation of carbon nanotube yarns, Smart Mater. Struct. 16 (2007) S243–S249.
[20] J. Foroughi, G.M. Spinks, G.G. Wallace, J. Oh, M.E. Kozlov, S. Fang, T. Mirfakhrai, J.D.W. Madden, M.K. Shin, S.J. Kim, R.H. Baughman, Torsional carbon nanotube artificial muscles, Science 334 (2011) 494–497.
[21] J.A. Lee, Y.T. Tae Kim, G.M. Spinks, D. Suh, X. Lepró, M.D. Lima, R.H. Baughman, S.J. Kim, All-solid-state carbon nanotube torsional and tensile artificial muscles, Nano Lett. 14 (2014) 2664–2669.
[22] J.A. Lee, N. Li, C.S. Haines, K.J. Kim, X. Lepró, R. Ovalle-Robles, S.J. Kim, R.H. Baughman, Electrochemically powered, energy-conserving carbon nanotube artificial muscles, Adv. Mater. 29 (2017) 1700870.
[23] R.H. Baughman, Muscles made from metal, Science 300 (2003) 268–269.
[24] M.D. Lima, S. Fang, X. Lepró, C. Lewis, R. Ovalle-Robles, J. Carretero-González, E. Castillo-Martínez, M.E. Kozlov, J. Oh, N. Rawat, C.S. Haines, M.H. Haque, V. Aare, S. Stoughton, A.A. Zakhidov, R.H. Baughman, Biscrolling nanotube sheets and functional guests into yarns, Science 331 (2011) 51–55.
[25] C.H. Kwon, S.H. Lee, Y.B. Choi, J.A. Lee, S.H. Kim, H.H. Kim, G.M. Spinks, G.G. Wallace, M.D. Lima, M.E. Kozlov, R.H. Baughman, S.J. Kim, High-power biofuel cell textiles from woven biscrolled carbon nanotube yarns, Nat. Commun. 5 (2014) 3928.
[26] M.D. Lima, N. Li, M.J. de Andrade, S. Fang, J. Oh, G.M. Spinks, M.E. Kozlov, C.S. Haines, D. Suh, J. Foroughi, S.J. Kim, Y. Chen, T. Ware, M.K. Shin, L.D. Machado, A.F. Fonseca, J.D.W. Madden, W.E. Voit, D.S. Galvão, R.H. Baughman, Electrically, chemically, and photonically powered torsional and tensile actuation of hybrid carbon nanotube yarn muscles, Science 338 (2012) 928–932.
[27] S.H. Kim, C.H. Kwon, K. Park, T.J. Mun, X. Lepró, R.H. Baughman, G.M. Spinks, S.J. Kim, Bio-inspired, moisture-powered hybrid carbon nanotube yarn muscles, Sci. Rep. 6 (2016) 23016.
[28] S.H. Lee, T.H. Kim, M.D. Lima, R.H. Baughman, S.J. Kim, Biothermal sensing of a torsional artificial muscle, Nanoscale 8 (2016) 3248–3253.
[29] J.A. Lee, M.K. Shin, S.H. Kim, H.U. Cho, G.M. Spinks, G.G. Wallace, M.D. Lima, X. Lepró, M.E. Kozlov, R.H. Baughman, S.J. Kim, Ultrafast charge and discharge biscrolled yarn supercapacitors for textiles and microdevices, Nat. Commun. 4 (2013) 1970.
[30] H.J. Sim, C. Choi, D.Y. Lee, H. Kim, J.H. Yun, J.M. Kim, T.M. Kang, R. Ovalle, R.H. Baughman, C.W. Kee, S.J. Kim, Biomolecule based fiber supercapacitor for implantable device, Nano Energy 47 (2018) 385–392.
[31] C. Choi, K.M. Kim, K.J. Kim, X. Lepró, G.M. Spinks, R.H. Baughman, S.J. Kim, Improvement of system capacitance via weavable superelastic biscrolled yarn supercapacitors, Nat. Commun. 7 (2016) 13811.
[32] C.S. Haines, N. Li, G.M. Spinks, A.E. Aliev, J. Di, R.H. Baughman, New twist on artificial muscles, Proc. Natl. Acad. Sci. U.S.A. 113 (2016) 11709–11716.
[33] C.S. Haines, M.D. Lima, N. Li, G.M. Spinks, J. Foroughi, J.D.W. Madden, S.H. Kim, S. Fang, M.J.D. Andrade, F. Göktepe, Ö. Göktepe, S.M. Mirvakili, S. Naficy, X. Lepró, J. Oh, M.E. Kozlov, S.J. Kim, X. Xu, B.J. Swedlove, G.G. Wallace, R.H. Baughman, Artificial muscles from fishing line and sewing thread, Science 343 (2014) 868–872.
[34] J. Liang, Y. Huang, J. Oh, M. Kozlov, D. Sui, S. Fang, R.H. Baughman, Y. Ma, Y. Chen, Electromechanical actuators based on graphene and graphene/Fe3O4 hybrid paper, Adv. Funct. Mater. 21 (2011) 3778–3784.